Two-dimensional position-sensitive silicon detectors for the ACE Solar Isotope Spectrometer

Mark E. Wiedenbeck[1], Eric R. Christian[2], Walter R. Cook[3],
Alan C. Cummings[3], Brian L. Dougherty[1], Richard A. Leske[3]
Richard A. Mewaldt[3], Edward C. Stone[3], and Tycho T. von Rosenvinge[2]

[1] Jet Propulsion Laboratory, Pasadena, CA 91109
[2] Goddard Space Flight Center, Greenbelt, MD 20771
[3] California Institute of Technology, Pasadena, CA 91125

ABSTRACT

Two-dimensional position-sensitive silicon detectors ("matrix detectors") have been designed, procured, and tested as part of the development of the Solar Isotope Spectrometer (SIS) instrument for NASA's Advanced Composition Explorer (ACE) mission. Important characteristics of these devices include: thickness ~ 50–$90\,\mu$m, active area $34\,\mathrm{cm}^2$, 64 strips on each surface with 1 mm strip pitch. The SIS instrument uses four such detectors, processing signals from each of the 512 individual strips with a separate 12-bit pulse height analyzer implemented with custom-designed VLSI circuits. A set of 25 matrix detectors have been characterized through a variety of tests intended both to select the best candidates for use in the flight instrument and to provide the calibrations needed to interpret flight data. We discuss the design of the SIS matrix detectors and present selected results from the detector tests that have been performed.

Keywords: silicon detectors, position-sensitive detectors

1. INTRODUCTION

The Solar Isotope Spectrometer (SIS) is one of nine instruments currently under development as the scientific payload for the Advanced Composition Explorer (ACE) mission. This instrument complement includes 6 major mass and/or charge spectrometers which, as a group, are able to study heavy nuclei over an energy range from $\sim 1\,\mathrm{keV/nucleon}$ to nearly $1\,\mathrm{GeV/nucleon}$. This payload will enable definitive studies of the abundances of nearly all isotopes from H through Zn ($1 \le Z \le 30$). Figure 1 shows the charge and energy ranges that will be studied with each of the ACE instruments. The scientific problems which will be addressed using these measurements have been reviewed by Stone *et al.*[1].

1.1 SIS measurement objectives

The SIS instrument is designed to provide elemental and isotopic resolution over the energy range from ~ 10 to $\sim 200\,\mathrm{MeV/nucleon}$. These measurements will be used in the study of solar energetic particles (SEPs), anomalous cosmic rays (ACRs), high energy particles accelerated in the interplanetary medium, and low-energy galactic cosmic rays.

1.2 The SIS instrument

To make the intended measurements, SIS uses a sensor system consisting entirely of silicon solid state detectors. The detectors are arranged in two identical "stacks", one of which is illustrated in Figure 2. Particle identification is based on measurements of a particle's energy loss, ΔE, and total energy, E, as it penetrates a detector (thickness L) and comes to rest in the remaining portion of the detector stack:

$$L \sec\theta = R_{Z,M}(E/M) - R_{Z,M}((E - \Delta E)/M), \tag{1}$$

where $R_{Z,M}$ is the tabulated range of a particle of atomic number Z and mass number M as a function of the particle's energy per nucleon. The $\sec\theta$ factor takes into account the increased path length traversed by a particle incident at an angle θ from the normal to the detector surface.

The bottom portion of the stack consists of 15 large-area ($65\,\mathrm{cm}^2$) silicon diodes from which the energy loss measurements (E and ΔE in Eq. 1) are obtained. These detectors are discussed in another paper at this conference[2]. The 9.1 cm total thickness of silicon in this stack establishes the upper energy limit of the SIS instrument.

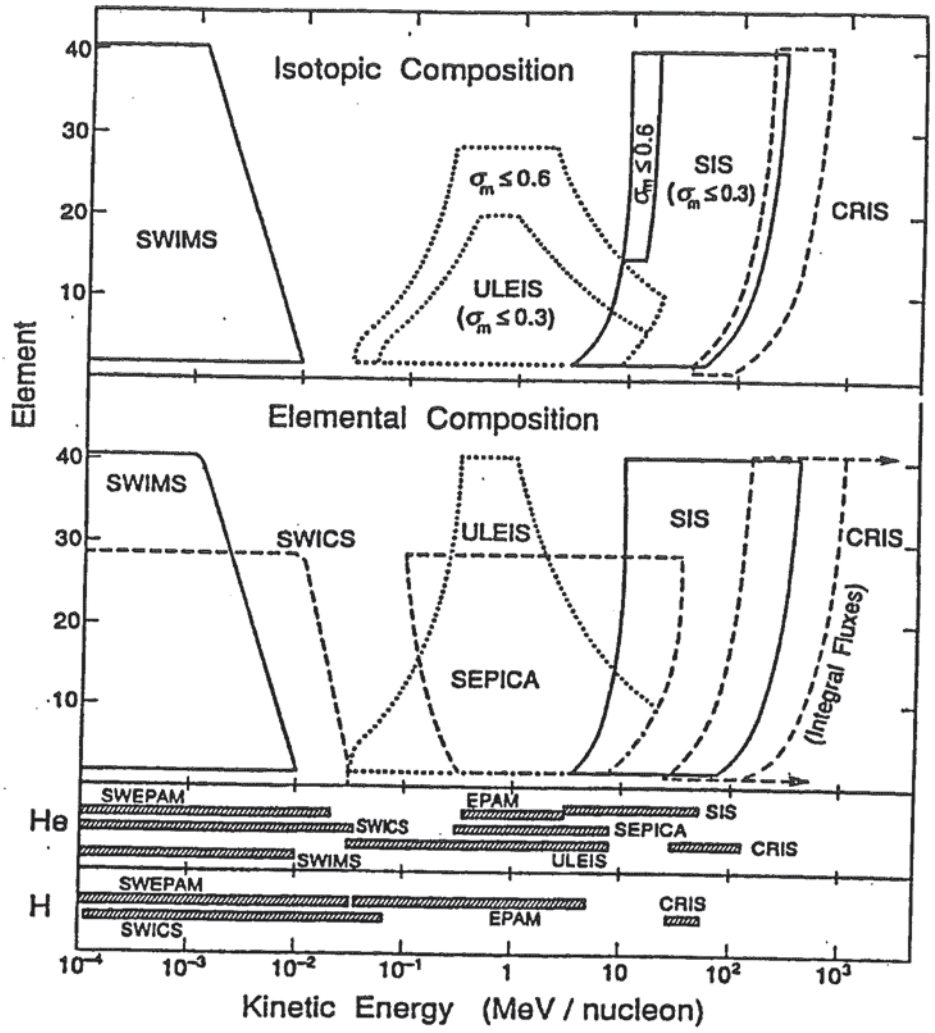

Figure 1. Range of energies and atomic numbers over which each of the ACE instruments will make measurements. The top panel shows the intervals over which isotopes will be resolved and the second panel shows the intervals for charge resolution. The bottom two panels show the energies over which hydrogen and helium will be measured.

In front of the energy loss stack the instrument requires a trajectory-measurement system capable of providing both the angle of incidence, θ, and the position at which each particle penetrates the subsequent detectors. This latter information is needed for making corrections for the spatial nonuniformities of the detector thicknesses and for eliminating background particles such as those which exit through the edge of the stack before coming to rest.

2. SIS "MATRIX" DETECTORS

2.1 Requirements and design

In SIS the trajectory system is implemented using pairs of two-dimensional position sensitive silicon detectors at the front of each stack. These devices, referred to as "matrix" detectors, have their front and back electrical contacts segmented into parallel strips with those on opposite surfaces running in perpendicular directions. Each surface has 64 strips with a 1 mm pitch and with gaps of 40 μm between adjacent strips. This strip geometry, together with the 6 cm spacing between the two matrix detectors, provides an rms angular resolution ~ 0.2–$0.3°$. With this resolution the contribution of the trajectory uncertainty to the errors in calculated particle masses will be less than

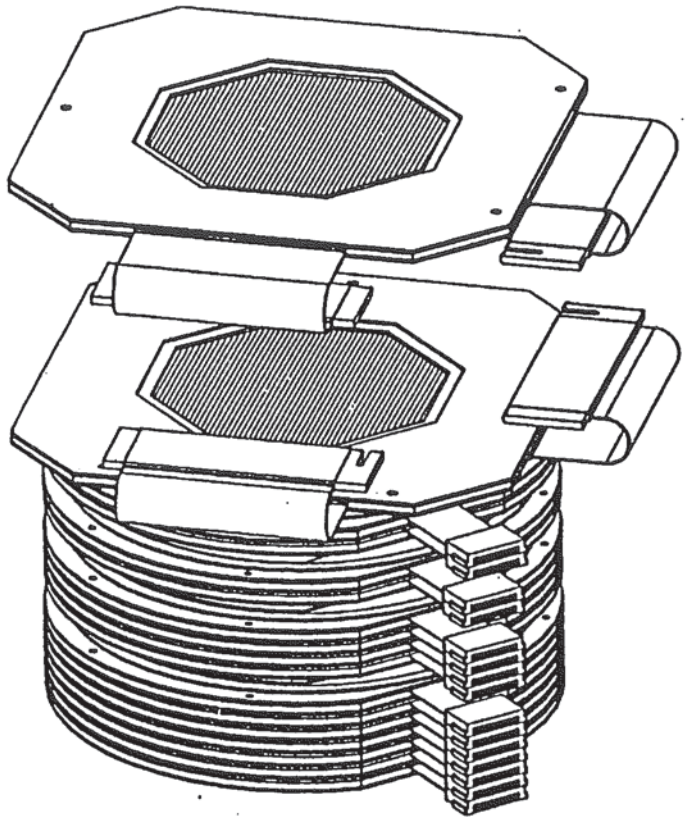

Figure 2. Illustration of one of the two silicon detector stacks used in the SIS instrument. The top two detectors are the matrix detectors discussed in this paper. The vertical separation of 6 cm between these two detectors provides the lever-arm needed to achieve the desired angular resolution, given the 1 mm pitch of the detector strips. Below the matrix detectors are 15 large-area detectors used for measuring particle energy losses.

the contribution from fundamental effects such as energy loss fluctuations, charge state fluctuations, and multiple scattering.

The low energy particle populations to be studied using SIS typically exhibit energy spectra which fall rapidly with increasing energy. Thus SIS is designed to have a relatively low threshold energy. This energy threshold is determined, primarily, by the amount of material a particle must penetrate in order to provide a set of signals sufficient to identify its charge and mass. High resolution measurements can be achieved for particles which penetrate the first detector (100 μm thick) in the energy loss stack and stop in the second detector. The combined thickness of the two matrix detectors should not be significantly greater than this 100 μm thickness. In fact, because the matrix detectors provide pulse height as well as trajectory information, it should be possible to identify many of the particles which stop in the first energy loss detector, or even in the second matrix detector. SIS was designed to use matrix detectors which are 60 ± 10 μm thick, although in the course of developing these detectors we tested devices ranging from 50 μm to 90 μm. With the nominal 60 μm matrix detector thickness ^{56}Fe nuclei require minimum energies of 13.3 MeV/nucleon or 19.2 MeV/nucleon to reach the first and second energy loss detectors, respectively (taking into account the thickness of the thin kapton window that covers the SIS instrument).

The SIS instrument needs to be able to make measurements during large solar energetic particle events in which the heavy nuclei of interest can be accompanied by intense fluxes of protons and alpha particles. Under these circumstances there is a high probability that more than one particle will enter the matrix detector within the resolving time of the instrument. This effect is particularly severe for the front matrix detector which has minimal overlying material to stop very low energy particles and which has a large unobstructed field of view. To work in this high-rate environment, each of the SIS matrix detector strips is instrumented with a separate pulse height analyzer. This reduces the area over which pile-up can occur by a factor ~ 50 (detector area/strip area). In some cases it should also allow us to select which of several coincident tracks through the matrix detectors produced the observed signals in the energy loss stack.

To produce the large number of pulse height analyzers needed for the SIS instrument (512 in all) within the power, size, and mass constraints of a spaceflight instrument, a custom CMOS VLSI circuit was developed. This

device, described by Cook *et al.*[3], contains 16 channels of charge sensitive amplifier (CSA), discriminator, sample-and-hold, and 12-bit Wilkinson run-down ADC. Four of these circuits are used for processing signals from the 64 strips on each surface of a matrix detector. Each strip is DC coupled to an amplifier input, and the VLSI circuits used to instrument the strips on the biased side of the detector are referred to the detector's bias voltage (in the range ~ 5 to 30 V) rather than to ground.

In addition to integrating the signals produced by the charged particles passing through the matrix detector, the CSAs also integrate the detector leakage current. This current is approximately canceled by the injection of a corresponding current of the opposite sign from a current-output digital-to-analog converter (IDAC). In addition, an electronic switch is periodically used to discharge the CSA's integration capacitor.

2.2 Detector fabrication

The SIS matrix detectors were fabricated by Micron Semiconductor Ltd., based on specifications developed by the SIS collaboration. As the starting material Micron used lapped and polished wafers cut from 75 mm diameter boules of high-resistivity n-type silicon. The use of 75 mm diameter silicon for the matrix detectors rather than 100 mm material such as that used for the detectors in the energy loss stack was dictated by considerations of the fragility of these thin wafers and the risk of breakage either during fabrication or during launch. Even with the 75 mm diameter material we experienced a rather low yield due to breakage during manufacture. The detector itself has an octagonal shape (see Fig. 2), which is a compromise between maximizing the usable detector area from the round diameter wafer and simplifying various fabrication operations.

Selective implantation of boron ions was performed on one surface of the detector to form the p-n junction and produce p-type strips separated by narrow n-type gaps. On the other (ohmic) surface, n^+ strips were produced using arsenic implants. Each surface of a matrix detector has a "guard ring" surrounding the active area containing the strips. This guard, which is left floating, is intended to reduce the leakage current to the strips.

A relatively high resistance ($\gtrsim 100\,\mathrm{k}\Omega$) is required between adjacent strips on both detector surfaces. There are small differences ($\lesssim 10\,\mathrm{mV}$) between the offset voltages at the inputs of the various CSAs, and when these voltage differences are imposed across the interstrip resistance they contribute to the leakage currents seen by the amplifiers. These currents must be kept small enough so that they can be nulled with the IDACs. In addition, when a particle produces ionization charge in the detector there is a voltage change on the hit strip (approximately the signal charge divided by the strip capacitance) which lasts until the CSA is able to respond by collecting the charge from the strip and returning it to its normal potential. While the strip's voltage is displaced from its steady state value some of the signal charge can flow to adjacent strips through the interstrip resistance. Thus the interstrip resistance should be made large to minimize this charge sharing between adjacent strips.

The implant structure on the junction side of the detector, p^+ strips separated by n-type gaps, tends naturally to produce the high resistance characteristic of a reverse biased diode structure. However, on the ohmic surface of the detector where we have n^+ strips implanted in n-type material the interstrip resistance depends critically on the resistivity of the silicon wafer. Commonly this resistance is smaller than the value required for good isolation of the strips. To increase the interstrip resistance on the ohmic side of the detector, Micron Semiconductor has used two different approaches. On some detectors they implanted an extra set of narrow p^+ lines centered along the gaps between the strips. This produces a pn diode structure similar to that on the junction side of the detector and tends to yield excellent isolation between strips. However it has proven difficult to accurately place this $\sim 10\,\mu$m wide line along the center of the $40\,\mu$m wide gap between strips because of the lack of sufficient flatness and stiffness of the thin detector wafers. In the other isolation technique, an estimate is made of the density of acceptor ions (typically boron) that must be implanted into the ohmic surface to balance the density of donors in the material and raise the surface resistivity to acceptable levels. Then the entire surface is implanted with a "boron spray" designed to achieve the appropriate acceptor density. While this technique can yield interstrip resistances in the range we need, it is difficult to control and often results in unacceptably low resistances.

Each completed matrix detector wafer was bonded into a G10 circuit board mount (Fig. 2) using a silicone compound. The coefficient of thermal expansion of the G10 is very similar to that of silicon, and the silicone is somewhat flexible, so the detectors can be operated over a wide temperature range without undue mechanical stress. Each strip on the detector was wire-bonded to a corresponding pad on the mount using two or three $25\,\mu$m aluminum wire bonds for redundancy. The detector mount is a multilayer structure in which one of the inner layers is a kapton "flexi-strip" used to bring out two sets of signal traces for connection to the external circuit board containing the

readout electronics. The mount is designed to have no electrical traces on the outer surfaces, allowing the mount to be precisely machined to the desired dimensions after it is fabricated by a printed circuit board vendor.

3. DETECTOR TEST PROGRAM

The completed matrix detectors were subjected to a variety of tests both at Micron Semiconductor and in our laboratory. These tests are intended to verify that the device characteristics meet the SIS requirements, to select the best of the available matrix detectors for flight, and to screen out any of the detectors which may be prone to failure during or after launch.

3.1 Operating bias, leakage current, and noise

Initially the strips on each surface of the detector are shorted together and measurements are made of the full-area characteristics of the device. Typical depletion voltages for the matrix detectors are ~ 4 to 6 V. At depletion the total leakage current typically is in the range 0.3 to 1.5 μa. Detector noise is measured using pulse shaping electronics with a peaking time $\sim 2.4\,\mu$s, to obtain a bandwidth comparable to that of the flight electronics. At depletion the noise is typically in the range 100 to 200 keV full width at half maximum (FWHM).

The maximum operating bias for these detectors tends to be poorly defined and to vary significantly from one device to another. In some cases the bias is limited by a sharp increase in the noise, while for others the noise shows no such abrupt increase but the leakage current continues to rise with increasing bias. If we impose a somewhat arbitrary limit of 10 μa on the overall leakage current, we find that maximum operating biases range from about 10 V for some detectors to greater than the 30 V limit of the flight bias supplies for others.

3.2 DC characteristics of strips

To determine whether the characteristics of the individual detector strips are compatible with the readout circuitry, a set of strip-by-strip DC measurements are made. First, all of the strips on the ohmic side are connected to ground through individual 10 kΩ resistors and all of the junction-side strips are connected through similar resistors to the desired bias voltage. The voltage drop across each resistor is measured with a high precision digital volt meter (DVM) and the leakage current is calculated. (Note that a 1 μa strip current through the 10 kΩ resistance causes only a 10 mV change in the voltage on the strip.)

To obtain a measure of the interstrip resistances, we use the same setup as described above but add a selected offset to the voltage applied to one strip at a time and measure how much the current for this one strip changes. We calculate a limit on the interstrip resistance by taking the ratio of the applied voltage offset to the change in current of the strip to which it is applied. This is done for several offset voltages ranging from 10 mV (typical of differences in the input offsets of the CSAs) to 1 V (approximately the largest voltage excursion expected on a strip due to a particle which produces a full-scale signal in the pulse height analyzer). These strip-by-strip measurements of leakage currents and resistances have been automated by using a computer to control a set of relays that make the necessary strip connections and commercial IEEE-488 instrumentation to apply the detector bias and strip offset voltage and to measure the voltage drops across the resistors.

Figure 3 shows a set of strip leakage current and resistance measurements made for one of the best matrix detectors we have studied. On this detector all of the strips have leakage currents well below the $\sim 1\,\mu$a limit of the IDAC, and all of the interstrip resistances exceed 1 MΩ. This particular detector was fabricated using a p^+ implant structure to achieve good strip isolation on the ohmic side.

On some detectors we find a small number of strips (one or two) with high currents—in extreme cases these strips account for most of the current measured for the entire detector. A more serious problem is encountered on many of the detectors fabricated using the boron spray isolation process. For these detectors we often find that nearly all of the strips on the ohmic side have resistances less than our 100 kΩ limit, sometimes so low that we can only tell that the resistances are less than the 10 kΩ resistors we use for making the current measurements. However, a few of the boron-spray detectors that we tested were found to have interstrip resistances comparable to those obtained using the p^+ implant structure.

3.3 Vacuum and temperature tests

In space the SIS detectors will operate in a hard vacuum within the temperature range −25C to 25C. In addition,

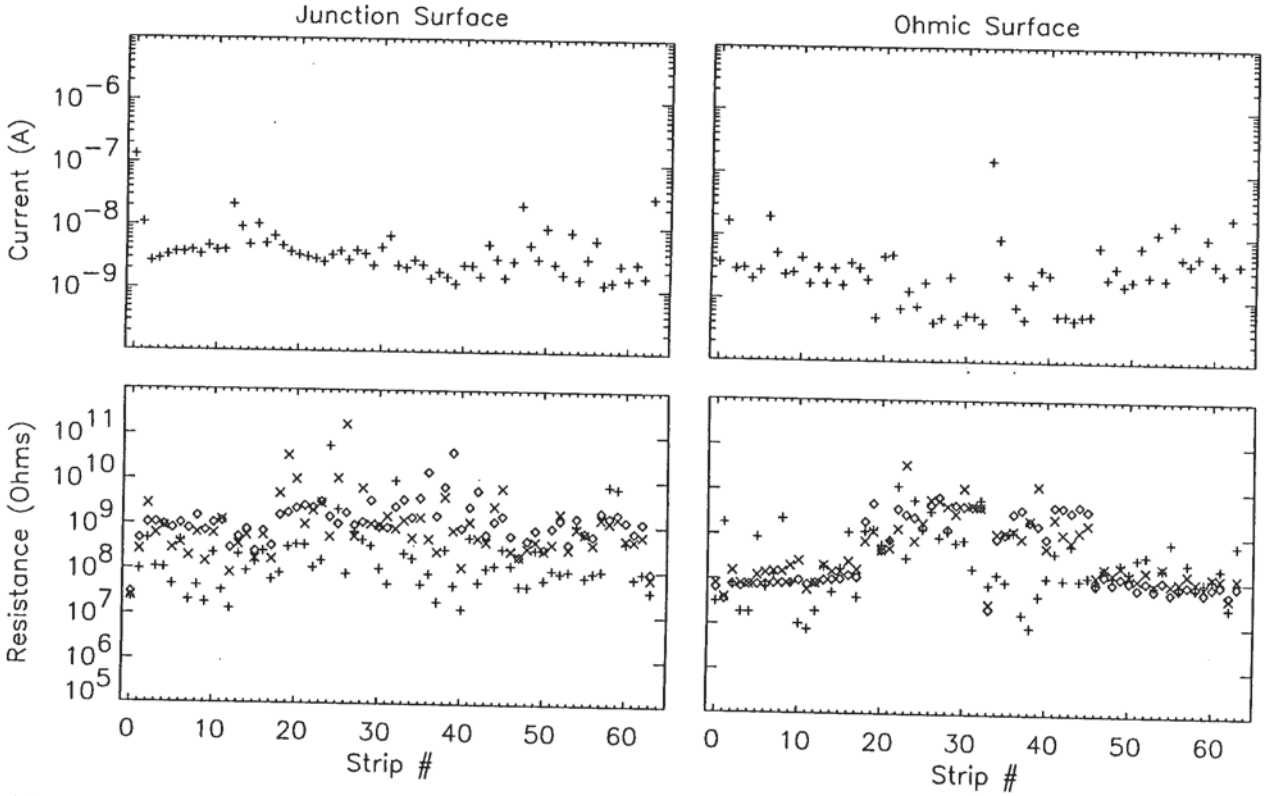

Figure 3. Measurements of DC characteristics made for one of the matrix detectors (PSD022). The panels on the left show measurements made on the junction surface of the detector and the panels on the right show measurements from the ohmic surface. The upper plots show the leakage current measured for each strip and the lower plots show the resistance between each strip and neighboring strips. All of these measurements were made with 7 V bias on the detector. The resistances were measured by applying voltage offsets of 0.01 V (+), 0.1 V (×), and 1 V (◇) to individual strips and measuring the change in the current for the offset strip.

they need to be able to survive (non-operating) without degradation over temperatures from −35C to 40C. A number of tests were performed to check that the devices could tolerate these conditions.

Micron Semiconductor carried out thermal cycling and thermal soak tests intended to reject marginal devices before we receive them. In the thermal cycling test the detectors were subjected, without bias, to 10 cycles between −40C and 40C. For the thermal soak test they were operated with bias for 24 hr at −40C and 168 hr at 40C. During the thermal soak the detectors were not continuously monitored, but leakage current measurements were made at several points in the test. Typically no problems were encountered during these tests.

At Caltech, sets of matrix detectors were put through a thermal–vacuum (TV) test with a duration of 2 to 3 weeks. A vacuum of $\sim 1 \times 10^{-6}$ torr was typically maintained. Following an initial several days at 20C the temperature was raised to 35C and maintained for at least a week. Near the end of the run the temperature was reduced to −25C for 1 to 2 days and then returned to room temperature. We had previously put the SIS energy loss detectors[2] (large area, single-area ion implanted detectors, also manufactured by Micron) through similar TV runs. With few exceptions those detectors proved very stable during the TV runs, showing essentially no changes except those associated with temperature-dependent variations of the leakage current. In contrast with this behavior, a number of the matrix detectors exhibited significant changes in their noise and/or leakage current in vacuum. Most commonly the noise level increased sharply when the matrix detector was first placed in vacuum, as compared with the noise measured in air at the same temperature. This elevated noise level tended to slowly drop over the course of the run, while exhibiting fluctuations by tens of percent over time scales of a few hours to a few days. The data suggest that the noise level is gradually becoming more stable over the course of the run, but a longer duration test

will be needed to adequately check this.

3.4 Vibration and acoustic tests

In order to assure that they will survive the vibration and acoustic environment to which they will be subjected during the ACE launch, the SIS matrix detectors have individually been tested to appropriate levels. The vibration tests were arranged by Micron Semiconductor and conducted by one of several British firms. The random vibration test had a duration of 1 minute and a power spectrum extending from 20 to 2000 Hz, with an overall amplitude of 15.2 g rms. Nearly all of the matrix detectors passed the vibration test without problems.

The acoustic level expected during the ACE launch, reaching $\sim$ 138 dB around 500 Hz, is particularly severe. In order to protect the thin matrix detectors the SIS instrument has a deployable cover which will be closed during launch. We have performed extensive acoustic tests to check the effectiveness of this cover in protecting the detectors and to verify that the detectors will be able to survive the acoustic loads they experience inside the closed instrument.

Tests of the effectiveness of the SIS acoustic cover indicated that the highest level that should be experienced by the matrix detectors inside the closed instrument is 132 dB, which occurs when the spacecraft is being qualified at 3 dB above the level anticipated for launch. Detectors were screened at a level of 135 dB. In all but a few cases the thin silicon wafers survived this acoustic level. However, on a number of detectors the acoustics caused the breakage of a significant number of the wire bonds used for electrical connection of the detector strips to traces on the printed circuit board mount. We were able to select a flight set of matrix detectors for which few, if any, wire bonds broke during the acoustic screening.

In the course of investigating acoustic effects on the matrix detectors Micron Semiconductor fabricated a number of devices using silicon wafers with a $\langle 100 \rangle$ crystal orientation rather than the $\langle 111 \rangle$ orientation we normally were using. The expectation was that this material should be mechanically stronger and therefore less susceptible to breakage due to the acoustic loads. In our acoustic screening tests, however, we have not seen a clear difference (up to 135 dB) in the performance of the wafers. Similarly, we have not observed a correlation of the problems experienced in the acoustic tests with wafer thickness. We suspect that the broken wire bonds are probably due to problems with the quality of the bonds rather than to the thickness of the wafer, particularly since detectors with bond-breakage problems commonly show indications of earlier failed bonding attempts on some of the pads.

3.5 Alpha particle tests

Tests with radioactive sources of alpha particles (^{244}Cm and ^{228}Th) were carried out to check the uniformity of each matrix detector's response and the uniformity of its dead layers. Most importantly, a coarsely collimated ^{244}Cm source was scanned over the detector, and pulse height spectra were measured at each of a large number of points distributed over the detector surface. We found the response to be completely uniform, to within the accuracy of the measurements. From the data we are able to set an upper limit of 0.2 μm (silicon equivalent) on the thickness variation of the dead layers. We have not yet derived the absolute thicknesses of the dead layers, but expect them to be no more than 2 μm based on information from Micron Semiconductor.

4. ACCELERATOR TESTS

The most detailed information about the matrix detector performance comes from accelerator tests of the flight instrument, since in this configuration the matrix detector is instrumented for measuring the pulse height on every strip. Two such accelerator tests have been done: a preliminary test was carried out at the Michigan State University (MSU) cyclotron in February 1996, and a more extensive test was done at the Gesellschaft für Schwerionenforschung (GSI) accelerator in Darmstadt, Germany in June 1996.

In the following paragraphs we discuss some of the initial results from the GSI run. For that test we used beams of ^{56}Fe at 300, 500, and 700 MeV/nucleon and ^{18}O at 300 MeV/nucleon. In addition, we used other nuclides produced from the primary beams by fragmentation in a CH_2 target.

4.1 Position measurements

When the SIS instrument is exposed to a parallel beam of heavy nuclei there should be a constant difference in the (x, y) locations at which the two matrix detectors in the telescope are penetrated. Thus a simple check of the detectors' position response can be obtained by looking at the distribution of differences between the two

locations. Figure 4 shows histograms of differences of the strip numbers with the maximum pulse heights in the two matrix detectors. These data were obtained from a run in which a 500 MeV/nucleon ^{56}Fe beam was degraded in energy and fragmented to produce a wide range of nuclei stopping throughout the entire depth of the energy loss stack. As expected, the position difference histograms contain sharp peaks centered at values consistent with those calculated from the direction of incidence of the beam. The widths of the peaks contain contributions due to the angular dispersion of the beam, which is caused by the accelerator's beam optics, multiple scattering in the degrader and target, and transverse momentum imparted to fragmentation products. We have not yet carried out a detailed comparison of observed and expected widths.

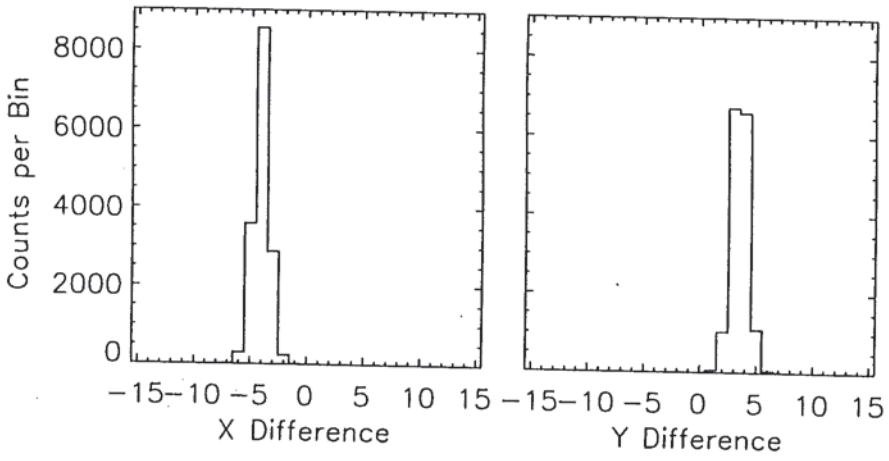

Figure 4. Histograms of measured coordinate differences in the two matrix detectors for an approximately parallel beam of particles. The coordinates used are just the numbers of the strips having the maximum pulse heights for each event.

4.2 Calibration of gains and offsets

The pulse height analyzers used for reading out the signals from the matrix detector strips have small but significant differences in their gains and offsets. In order to obtain precise energy loss information from the detector these quantities need to be accurately determined for each strip.

Whenever a particle was analyzed in the SIS instrument during the calibration, signals were measured from all of the matrix detector strips in the detector stack. In a normal event only a few strips have actually been stimulated, and the pulse heights read out from the rest of the strips correspond to the offsets of the electronics used for those strips. Thus the offset for a strip can be determined by simply taking the mean of a set of pulse heights measured for that strip when it is not hit. (In flight, strip offsets will periodically be measured on board and transmitted to the ground.)

The intercalibration of pulse height analyzer gains is simplified by the fact that each good particle event stimulates a strip on each surface of the detector. If one selects events which hit a particular strip on the front surface and then compare the pulse height measured on this strip with that measured on whichever strip was hit on the back surface, one can derive the gains of all the back-surface strips relative to the selected front-surface strip. Reversing the process and selecting a particular strip on the back extends the calibration to the rest of the front-surface strips. This procedure has the advantage that it is insensitive to thickness variations across the detector and to the identity of the detected particle. The determination of the absolute gain factor (a single number for each matrix detector) is complicated by the fact that measured signals depend both on this gain and on the detector's absolute thickness.

Figure 5 shows a set of relative gains derived for one of the matrix detectors using data obtained at GSI with an ^{56}Fe beam which had been degraded in energy and fragmented to produce a wide range of nuclei stopping throughout the SIS detector stack.

4.3 Detector thickness variations.

In order to achieve isotope resolution for heavy nuclei it is necessary to determine precisely the path length of each particle through the detector in which the energy loss measurement is made. The matrix detector thickness varies significantly (at least several percent) over the wafer surface, so it is necessary to measure these thickness variations and correct for them in the analysis of the flight data.

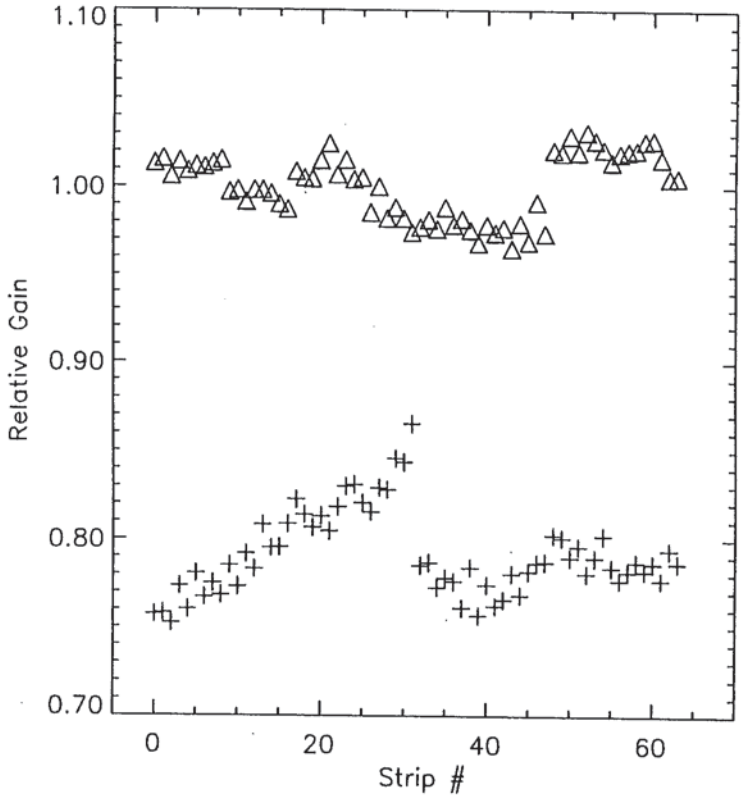

Figure 5. Relative gains derived for each of the strips on one matrix detector from data collected using a beam of ^{56}Fe plus fragmentation products. Gains shown with + 's are for strips on the junction surface and those shown with △'s are for strips on the ohmic surface. For this analysis, the offsets of all the pulse height analyzers (PHAs) were measured and subtracted. Nonlinearities in the PHA transfer function have not yet been taken into account, but analysis was restricted to a pulse height range over which they are not significant.

The active thickness (physical thickness minus dead layer thickness) can be derived from the energy losses measured for high energy particles which have ranges much larger than the matrix detector thickness. For these particles dE/dx is essentially constant in traversing the matrix detector, so the measured energy loss, ΔE, is proportional to the thickness. Figure 6 shows a map of mean energy loss signals from one of the matrix detectors for ^{36}Ar nuclei with an energy of 60 MeV/nucleon from the MSU cyclotron. The 1 MeV contour interval of this map corresponds to a change in the active thickness by approximately 1.5 μm. Thus the overall active thickness variation of the detectors is $\sim 5.5\,\mu$m, or 7% of the total thickness of this 77 μm thick device. Maps such as the one in Figure 6 should allow us to precisely derive the detector thickness penetrated by each particle.

4.4 Energy resolution

In order to allow identification of those particles which stop in either the second matrix detector or the first energy-loss detector, it is necessary to use the matrix detector pulse heights to provide the dE/dx measurements. While this use of the matrix detectors for energy loss measurements is secondary to their use for trajectory determination, it is important because it makes possible a significant reduction in the instrument's energy threshold for particle identification.

The gaps between strips on the matrix detectors are made narrow (40 μm) in order to minimize the fraction of the detector volume in which there may be a low electric field and associated loss of signal. In addition, since pulse heights are measured from both surfaces of the detector, the two signals can be compared for consistency. Figure 7 is a histogram showing the ratio of the pulse heights from the two surfaces of one of the matrix detectors after corrections have been made for the gains and offsets of all the strips. The distribution, which contains events covering a wide range of elements and energies, has a full width at half maximum of 0.6%. From this width of the ratio distribution, we estimate that the energy loss in the matrix detector can be measured to an accuracy of $\lesssim$0.2% when the signals from the two surfaces are averaged. This resolution should be adequate for measuring the masses of nuclei stopping in the shortest ranges of the SIS instrument.

We have not yet measured the mass resolution which can be obtained when using the matrix detectors to provide the energy loss measurement. However, in Figure 8 we show a plot of the pulse height measured in the second matrix detector versus the total energy deposited in the energy loss stack for particles which stop in the stack. The matrix detector pulse heights have been corrected for differences in relative gain, but no correction has been made for

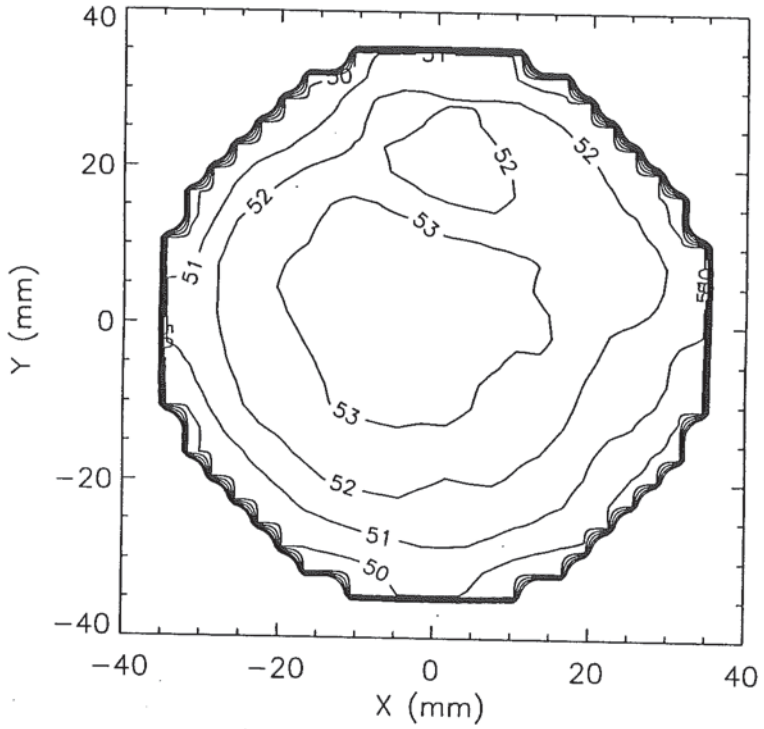

Figure 6. Map of energy losses in one of the matrix detectors (PSD022) as a function of position for a beam of ^{36}Ar nuclei at 60 MeV/nucleon. Energy loss variations reflect variations in the active thickness of the detector. Contours are labeled in MeV, and the contour interval of 1 MeV corresponds to a thickness change of approximately 1.5 μm.

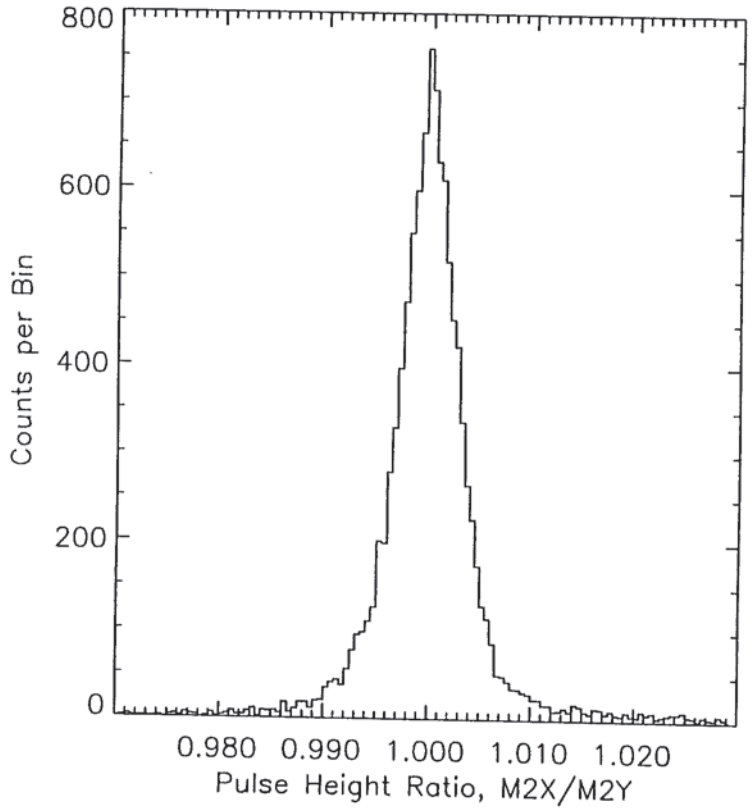

Figure 7. Histogram of the ratio of the pulse heights measured on the surfaces of one matrix detector for ^{56}Fe and its fragmentation products stopping at all depths in the SIS detector stack. The FWHM of the peak is 0.6%. Assuming that fluctuations in the two measured signals are equal and uncorrelated we calculate an rms error of 0.18% for each of the two measurements and 0.13% for their average. This provides an estimate of the pulse height measurement error which is independent of both detector thickness variations and Bohr / Landau fluctuations of the energy loss in the detector.

thickness variations of the matrix detector. The plot clearly shows element tracks for the primary iron beam and for a variety of lighter elements that were produced by fragmentation. Such charge measurements will be useful both for identifying particles at the low end of the SIS energy range and for enabling intercomparison with other signals from other detectors for background rejection.

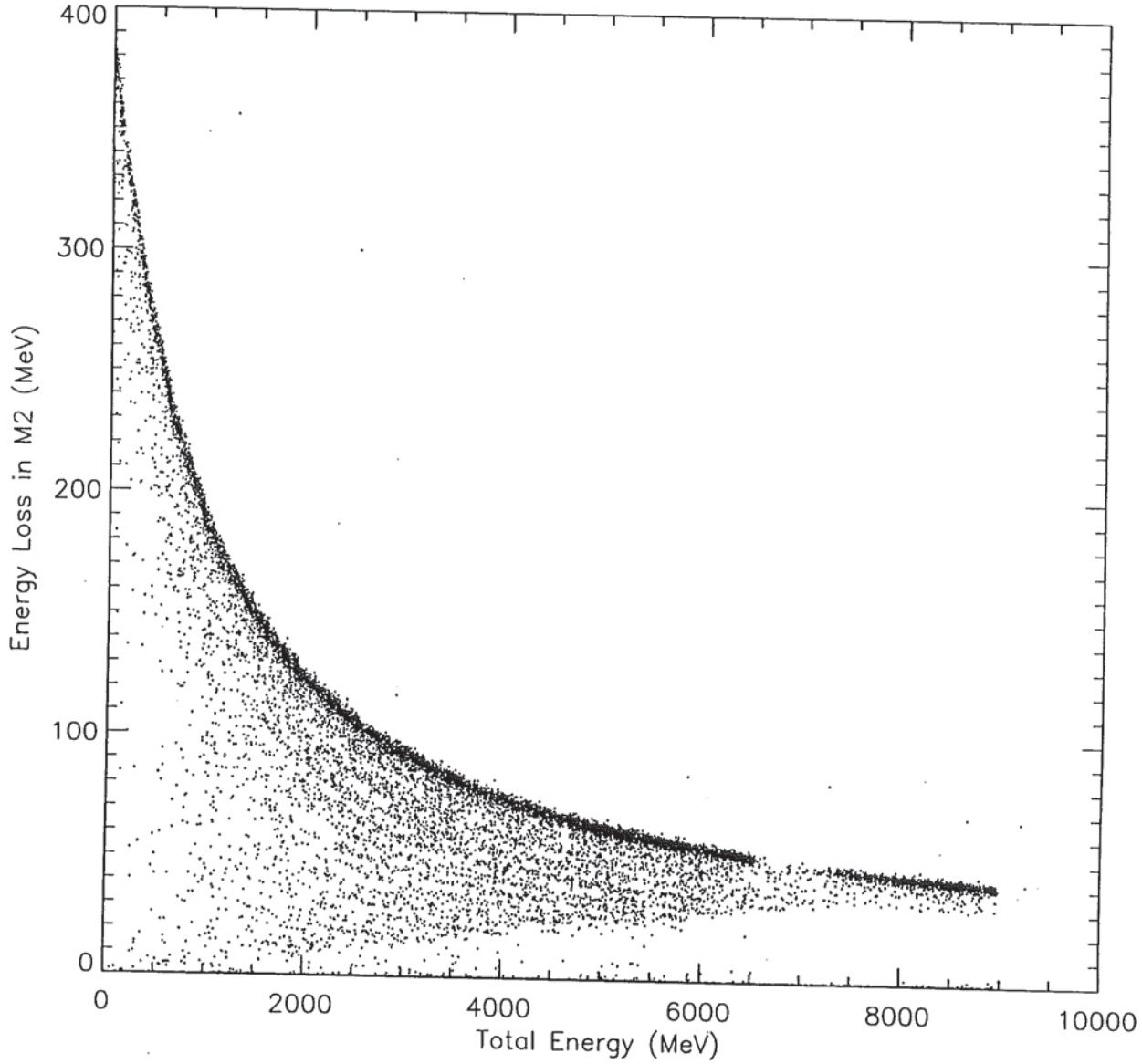

Figure 8. ΔE vs. total energy plot using the signal from the second matrix detector as ΔE. The matrix detector signals have been corrected for gain and offset differences between the strips, and the signals from the two surfaces of the detector have been averaged. No correction has been made for thickness variations of the matrix detector. The total energy signal is obtained by summing the signals from all of the detectors in the energy loss stack. The iron track includes particles stopping at all depths in the stack. A cut has been made to eliminate particles which penetrate the entire stack. Element tracks can be seen for the primary iron beam and for fragments produced from it. The origin of the data gap near the high-energy end of the iron track is currently being investigated.

4.5 Cross-talk between strips

Because the matrix detector strip pitch (1 mm) is significantly greater than both the gap between strips (40 μm) and the detector thickness ($70 \pm 20\,\mu$m), most particles passing through the detector should produce a signal on only a single strip on each surface. However, as discussed above (Section 2.2) the finite resistance between strips can cause some leakage of charge from the hit strip to adjacent strips during the time it takes for the charge sensitive amplifier to respond. To check the size of this effect we have looked at the pulse heights measured on the strips adjacent to

the hit strip for some of the heavy ion events collected during the MSU and GSI accelerator runs. In one test that was done using a detector known to have relatively low interstrip resistances ($\sim 100\,\mathrm{k}\Omega$) we were able to observe a small (percent level) charge leakage. In the higher resistance detectors that have been selected for flight the effect is clearly less. A preliminary analysis of ^{56}Fe beam data from GSI indicates that the typical charge leakage to adjacent strips is $< 0.2\%$.

5. PRESENT STATUS

The Solar Isotope Spectrometer has now been fully assembled and is scheduled for instrument-level environmental testing (vibration and thermal-vacuum) and then delivery to the ACE spacecraft team at the Johns Hopkins University Applied Physics Laboratory in September 1996. ACE is scheduled for launch in August 1997 into a halo orbit about the L1 Lagrangian point in the Sun–Earth system, 1.5 million kilometers sunward from the Earth.

We are continuing the analysis of accelerator calibration data and will be doing further testing of spare matrix detectors in order to assure the availability of replacements for those in the flight instrument, should that become necessary. Micron Semiconductor is in the process of fabricating additional detectors using a slightly modified design which may help improve the yield of matrix detectors having good isolation between strips.

6. ACKNOWLEDGMENTS

This research was supported by the National Aeronautics and Space Administration at the California Institute of Technology (under contract NAS5–32626 and grant NAGW–1919), the Jet Propulsion Laboratory, and the Goddard Space Flight Center. We wish to acknowledge C. Wilburn, A. Lucas, and the rest of the personnel at Micron Semiconductor for their close cooperation and very significant efforts in developing state-of-the-art position sensitive silicon detectors for SIS. We are grateful to the staffs of the GSI and MSU accelerators, and particularly to D. Schardt and N. Anantaraman, for their support of the SIS calibrations. We thank D. Aalami, G. Allbritton, B. Gauld, B. Kecman, S. Kleinfelder, M. Madden, H. Marshall, B. Milliken, R. Radocinski, B. Sears, and S. Shuman for their contributions to various aspects of developing and testing the matrix detectors and associated electronics.

7. REFERENCES

1. E. C. Stone, L. F. Burlaga, A. C. Cummings, W. C. Feldman, W. E. Frain, J. Geiss, G. Gloeckler, R. E. Gold, D. Hovestadt, S. M. Krimigis, G. M. Mason, D. McComas, R. A. Mewaldt, J. A. Simpson, T. T. von Rosenvinge, and M. E. Wiedenbeck, "The Advanced Composition Explorer", *The NASA Cosmic Ray Program for the 1990's and Beyond*, W. V. Jones, F. J. Kerr, and J. F. Ormes (eds.), pp. 48–57, Am. Inst. Phys. (Conf. Proc. #203), New York, 1990.

2. B. L. Dougherty, E. R. Christian, A. C. Cummings, R. A. Leske, R. A. Mewaldt, B. D. Milliken, T. T. von Rosenvinge, and M. E. Wiedenbeck, "Characterization of large-area silicon ionization detectors for the ACE mission", *Gamma-Ray and Cosmic Ray Detectors, Techniques, and Missions*, Vol. 2806, SPIE, 1996.

3. W. R. Cook, A. Cummings, B. Kecman, R. A. Mewaldt, D. Aalami, S. A. Kleinfelder, and J. H. Marshall, "Custom Analog VLSI for the Advanced Composition Explorer (ACE)", *Small Instruments for Space Physics*, B. T. Tsurutani (ed.), NASA, 1993.